Supplementary information

Signal-amplified surface-enhanced Raman scattering using core/shell satellite nanoparticles for norovirus detection

Enoch Y. Park,[1,2,†,*] Syuei Maehata,[2] Indra Memdi Khoris,[1,‡] Ojodomo Achadu[3]

[1] Research Institute of Green Science and Technology, Shizuoka University, 836 Ohya Suruga-ku, Shizuoka 422-8529, Japan

[2] Graduate School of Integrated Science and Technology, Shizuoka University, 836 Ohya Suruga-ku, Shizuoka 422-8529, Japan

[3] School of Health and Life Sciences, & National Horizon Centre, Teesside University, TS1 3BA, Middlesbrough, United Kingdom

E-mail address

park.enoch@shizuoka.ac.jp (EYP)

maeshuei0908@outlook.jp (SM)

imemdy95@gmail.com (IMC)

O.Achadu@tees.ac.uk (OA)

[*] Correspondence to: Research Institute of Green Science and Technology, Shizuoka University, 836 Ohya Suruga-ku, Shizuoka 422-8529, Japan.
E-mail address: park.enoch@shizuoka.ac.jp (E.Y. Park)

Present address:
[†] Faculty of Agriculture, Shizuoka University, 836 Ohya Suruga-ku, Shizuoka 422-8529, Japan
[‡] National Institute Advanced Industrial Science and Technology (AIST), Tsukuba, Ibaraki, 305-8565, Japan

S1 Experimental methods and materials

S1.1 Materials

4-Mercaptbenzoic acid (4-MBA) (1074-36-8, L(-)ascorbic acid (200-066-2), and N-hydroxysuccinimide (NHS) (B0249) were purchased from Tokyo Chemical Industry (Tokyo, Japan). Gold (III) chloride trihydrate (520918) and 1-ethyl-3-(3-dimetylaminopropyl) carbodiimide (EDC) (130672) purchased from Sigma (Tokyo, Japan). Carboxyl super Mag magnetic beads, 50 nm and 100 nm (SC0050-2) were purchased from Ocean Nanotech (San Diego, USA). Other reagents not specifically mentioned in this manuscript were purchased from FUJIFILM Wako Pure Chemical Corporation, Osaka, Japan. The screen-printed gold electrode (C220BT, Metrohm Japan, Tokyo, Japan) was used as SERS substrate.

Anti-NoV antibody broadly reactive to genogroup II (NS14 Ab), which is specific and broadly reactive to genogroup II of NoV, was provided by Professor T. Suzuki of Hamamatsu University School of Medicine. Norovirus-like particles (NoV-LPs) were expressed in the baculovirus expression system and purified following our laboratory's virus-like particle preparation protocol. Clinically isolated NoVs from fecal samples of the patients with infectious gastroenteritis were provided by Dr. F. Abe of Environment and Hygiene Institute in Shizuoka Prefecture. The NoV concentration of the supernatants was determined to be G II 4: 5.7×10^7 RNA copy number/mL by RT-PCR. The fecal matter of a single human donor (991-18) was purchased from Lee Biosolutions (MO, USA). Recombinant dengue virus 2 NS1 protein (ab181966) was purchased from Abcam (Cambridge, UK). Anti-mouse IgG-HRP was purchased from Santa Cruz Biotechnology (CA, USA). SARS-CoV-2 (COVID-19) Spike (D614G variant) protein and His tag

(GTX02575-pro) were purchased from Funakoshi (Tokyo, Japan). Influenza virus H1N1 New Caledonia was purchased from iha-003-b (Rehovot, Israel). Zika virus lysate (PRVABC59 Strain) was obtained from The Native Antigen Company (Oxfordshire, UK). Human serum (from human male AB plasma) (H4522) was obtained from Sigma (Tokyo, Japan).

S1.2 Synthesis of AuNPs and nanotag (Au@Ag-MBA-Au)

AuNPs and Au@Ag core-shell nanoparticles were synthesized according to our laboratory method [1]. Briefly, 500 µL of AuNP solution was prepared by mixing 250 µL of AuNPs and 250 µL of deionized (DI) water; 1 mL of AuNP solution was mixed with 1 mL of $AgNO_3$ and hydroquinone (HQ) (1:1v/v) in a 1.5 mL tube for 5 min at room temperature. The color changed from red to orange. The reaction solution was centrifuged at 2500 g for 5 min, and the resulting precipitate was redissolved in 1 mL of DI water. Since the supernatant changed to orange, it was further centrifuged at 6500 g for 10 min, and the resulting precipitate was redissolved in the previous solution. Finally, the supernatant was centrifuged at 8500 g for 15 min to redissolve the precipitate, a clear Au@Ag solution.

To conjugate the Raman molecule 4-MBA on the Au@Ag surface, 10 µL of 1 mM 4-MBA was added to 1 mL of Au@Ag solution, and the mixture was stirred at room temperature for 6 h. After the reaction, centrifugation was performed in the same steps as previously described, but the precipitate was redissolved in 1 mL of polyvinylpyrrolidone (PVP) (1 mM) to obtain Au@Ag-MBA. The synthesis of Au@Ag-MBA-Au was performed following the method [2]. Briefly, to 1 mL Au@Ag-MBA solution, 200 µL of 10 mM L(-)ascorbic acid was added, and the pH was adjusted to 12 with 0.1 mM NaOH.

Then, 280 μL of $HAuCl_4$ solution (0.05, 0.1, 1, and 1.5 mM) was added at a rate of 10 μL/min with constant stirring. The color of the solution changed from orange to a mixture of orange and red, and the solution was then stirred for 30 min, centrifuged, and redissolved in 1 mL of phosphate-buffered saline (PBS) buffer to obtain the novel nanotag (Au@Ag-MBA-AuNPs). The nanotag was stored at 4°C until use.

S1.3 Structural and optochemical characterization

The structural, optical, and physicochemical properties of AuNPs, Au@AgNPs, and Au@Ag-MBA-AuNPs were investigated. The particle morphology was examined by transmission electron microscopy (TEM) (JEM 1400 Plus, JEOL, Tokyo, Japan). Elemental mapping was performed using a scanning transmission electron microscope (STEM) (JEM-2100F, JEOL, Tokyo, Japan). Absorption spectra were measured using a fluorescence measuring instrument (Infinite M200, TECAN, Switzerland). Particle shape and zeta potential were measured in DI water using a Malvern Zetasizer (Nano-ZS, Malvern, UK) in a transparent disposable zeta cell (DTS1061, Malvern Panalytical, Spectris Co. Ltd., Surrey, UK). Raman scattering was measured using a laser Raman spectrometer (NRS-5500, Jasco, Tokyo, Japan) or a Palmtop Raman spectrometer (PR-1w, JASCO, Tokyo, Japan). The detail specification described in **Table S1**. Big difference in between these two Raman spectrometers is instrument size: the former is 880 (W) × 890 (D) × 670 (H) mm, 200 kg and the latter, 85 (W) × 222 (D) ×38 (H) mm, 0.8 kg.

S1.4 Anti-NoV antibody conjugation on MNP and nanotag

1 mL of 0.1 mg/mL MNP solution was prepared, and 500 μL of 0.1 M EDC solution in

2-morpholinoethanesulfonic acid, monohydrate (MES) buffer was added for carboxyl group activation and stirred for 30 min. Then 500 μL of 0.1 M *N*-hydroxysuccinimide (NHS) solution in MES buffer was added and stirred for another 1 h. After the reaction, 8 μL of 0.3 mg/mL anti-NoV antibody was added, and the antibody conjugation reaction was carried out for 1 h. The mixture was washed with DI water, dissolved in 1 mL of 2% BSA solution for blocking, and agitated for another 1 h. Finally, the samples were washed with DI water to remove BSA, redispersed in 1 mL of PBS, and stored at 4°C until use.

In the case of the nanotag, 1 mL of nanotag and 5 μL of 0.3 mg/mL anti-NoV antibody were added, and the mixture was stirred at 4°C for 6 h. Then, 100 μL of 2% BSA solution was added for blocking, and the mixture was agitated for another 1 h. Finally, the anti-NoV antibody-modified nanotags (Ab-Au@Ag-MBA-AuNPs) were centrifuged, redissolved in 1 mL of PBS, and stored at 4°C until use.

S1.5 Confirmation of antibody modification by ELISA

One hundred μL of antibody-modified MNPs (Ab-MMPs) were added to 500 μL of a 5000-fold diluted anti-mouse IgG-HRP. After 30 min of incubation under room temperature, the samples were washed with PBST (containing 0.1% Tween 20 in PBS buffer) using magnetic separation. After washing, 3,3',5,5'-tetramethylbenzidine (TMB) (100 μl), a chromogenic substrate, was added to the well as a coloring reagent, and the solution appeared blue due to the reaction. The reaction was then stopped by adding 50 μL of 10% H_2SO_4, which changed the color of the solution from blue to yellow. The absorbance of the solution was measured using a microplate reader at 450 nm with a reference filter of 655 nm. Antibody unmodified MNPs were used as controls.

Fifty μL of antibody-modified nanotags (Ab-nanotags) were added to 96 well plates

and immobilized at 4°C overnight. After washing, 200 μL of 5% scheme milk was added and left at 4°C for at least 6 h. After washing with PBST, 100 μL of anti-mouse IgG-HRP diluted 5000-fold in 2% BSA was added and incubated for 1 h at 37°C in a plate shaker. After washing, followed the previous Ab-MMPs protocol. The antibody-unmodified nanotag was used as a control for comparison.

S1.6 Norovirus detection

To investigate the conditions for the most sensitive virus detection using the employed handheld Palmtop Raman spectrometer (PR-1w, JASCO, Tokyo, Japan), 10 pg of NoV-LP was measured, varying the size of MNPs (50 nm and 100 nm) and incubation time (5–30 min), under measuring conditions of laser power of 5 mW and exposure time of 1 sec. 50 μL of antibody-modified nanotag, 50 μL of Ab-MNP, and 100 μL of NoV-LP were mixed in a 1.5 mL Eppendorf tube and incubated at 37°C for 30 min to form a sandwich structure of Ab-nanotag, Ab-MNP and NoV-LP. After sandwich forming by NoV-nanotag-MNP, supernatant was separated using a magnet to collect the analyte. Then, the samples were washed twice with PBST using magnetic separation and redissolved in 5 μL of PBS to remove unreacted Nanotag. The Samples were then dropped onto a gold substrate placed on a magnet, and Raman scattering was measured using a laser Raman spectrometer (NRS-5500, Jasco, Tokyo, Japan) or a Palmtop Raman spectrometer (PR-1w, JASCO, Tokyo, Japan).

The NoV-LP (0.01 pg/mL to 100 ng/mL) was detected using a commercial NoV detection kit (NV-EIA, Denka Co. Ltd., Niigata, Japan), and the sensitivity was compared with this study's.

S1.7 Selectivity and stability of detection signal in interfering agents

To confirm the detection selectivity, NoV-LP (100 fg), 100 pg of Dengue virus NS1 protein, H1N1 Influenza virus, SARS-CoV-2 S-protein, and Zika virus were detected under the previous detection protocol.

Five sample solutions were prepared for detection to examine the detection stability in the interfering agents, and the result was represented as the coefficient of variation (CV, %) (standard deviation/mean value × 100). 100 μL of 0.1 pg, 1 pg, and 10 pg NoV-LP were measured in the interfering agents, PBS, 10% and 30% human serum, and 10% feces according to the previous detection protocol.

S2 Operation of Raman spectrophotometer and measurement conditions

Two equipments with different measurement modes were used for the SERS study - the laser Raman spectrophotometer and Palmtop Raman spectrophotometer (**Supplementary Table S1**). The laser Raman spectrometer (**Table S1a**) is characterized by its ability to change the laser wavelength and its high resolution, while the Palmtop Raman spectrometer has a handheld size, similar to a smartphone (**Table S1b**). To investigate the optimal measurement conditions for the laser Raman spectrometer, the laser wavelength was set at 785 nm with the objective lens magnification switched between × 5, × 20, and × 100. As a result, only a small amount of SERS measurements could be done with the × 5 objective lens magnification, while SERS could be measured with higher intensity with the × 20 and × 100 objectives, showing the intensity at 1078 cm^{-1} and the × 20 objective lens magnification was able to measure higher intensity (**Fig. S3a–b**). When the Raman spectra at laser wavelength of 785 and 532 nm fixed × 20 objective lens

magnification show the specific 1078 cm^{-1} and 1585 cm^{-1} peaks of 4-MBA and the peak intensity was found to be higher at 532 nm (**Fig. S3c**). Since higher energy excitation light scatters more, we can say that the Raman scattering intensity was higher at 532 nm.

However, since the laser wavelength of 532 nm was not employed in the Palmtop Raman, and the laser wavelength of 785 nm and an objective lens magnification of × 20 were used for the Palmtop Raman spectrometer. The nanotags were measured at different laser outputs of 5 mW, 25 mW, and 50 mW, but the 4-MBA peak was identified at 5 mW and 25 mW (**Fig. S4a**). At 50 mW, the 4-MBA peak could not be confirmed, maybe because the laser power was too strong, and the substrate peak prevailed to the 4-MBA. Next, the laser power was set to 25 mW, and the exposure time of the excitation light was changed to 0.1, 0.2, 0.5, 1, 1.5, and 2 sec for the nanotag measurement. The 4-MBA peak could be observed at all exposure times, and the SERS intensity increased with exposure time (**Fig. S4b, c**). It is desirable to be able to measure at as short an exposure time as possible since long exposure times can have significant damage to the sample. Therefore, in actual NoV detection, laser output and exposure time were set according to the sample.

Comparing the laser Raman spectrometer and Palmtop Raman spectrometer, the laser Raman spectrometer is equipped with a microscope so that the measurement position can be selected by actual observation, and the focus can be easily adjusted. In practical virus detection, the laser Raman spectrometer has too many points that can be measured, and if the sample is not dropped evenly onto the substrate, the results will vary greatly depending on the measurement location, and the measurement time will be very long. However, with the Palmtop Raman spectrometer, it is always possible to measure at the same point if a holder corresponding to the substrate is used, and there is no need to worry about the uniformity of the sample. Also, in the case of virus detection, MNP makes it

possible to always condense the sample at the same point on the substrate, thus increasing reproducibility. And because the measurement time is very short, less than one minute, a Palmtop Raman spectrometer was more convenient for actual NoV detection.

S3 SERS Enhancement factor [3] determination

The SERS enhancement factors (EFs) of the Au-MBA, Au@Ag-MBA and Au@Ag-MBA-Au nanotags were determined using Eqn. (1):

$$EF = \frac{{}^{I_{SERS}}/_{N_{SERS}}}{{}^{I_{Norm}}/_{N_{Norm}}} \qquad (1)$$

where I_{SERS} and I_{NORM} are the intensities of the characteristic peaks of the nanotags or 4-MBA at 1078 cm^{-1} in the SERS and normal Raman measurements, respectively; N_{SERS} and N_{NORM} are the number of molecules (adsorbed on the NPs) responsible for the Raman signals in SERS or normal Raman measurements, respectively.

S4 Optimization of the biosensor materials components for NoV-LP detection

To achieve the most sensitive NoV detection, the size and amount of the MNP used for the detection were investigated. Two different sizes of MNP (50 nm and 100 nm) were used for NoV detection, and there was not significant difference in the signal, but Raman intensity using 50 nm MNP was higher than that using 100 nm MNP (**Fig. S5a**). When three different volumes of MNP (25, 50, and 75 μL) were used fixing the MNP size of 50 nm, the Raman intensity was increased with the increase of MNP volume (**Fig. S5b**). On the other hand, for the control sample, there was no change in the Raman intensity

between 25 µL and 50 µL, but around two times increased at 75 µL. It means that the MNP may bind with nanotags nonspecifically. Therefore, 50 µL of 50 nm MNP was used for NoV detection. The incubation time was optimized by changing the incubation time to 5–30 min and found that the Raman intensity increased significantly from 20 min and further increased at 30 min (**Fig. S5c**). Therefore, in this study, we incubated 30 min for NoV detection. When samples were dropped on the substrate without a magnet, a coffee ring was observed (below image in **Fig. S5d**), and no change in Raman intensity was observed (**Fig. S5d**) because there were no nanotags in the center. On the other hand, using a magnet to drop onto the substrate suppressed the coffee ring formation (above image in **Fig. S5d**). Since the laser of the Palmtop Raman spectrometer measures SERS by focusing it on the center of the gold substrate, a concentration-dependent increase in Raman intensity was observed from 10 fg to 10 pg. This result shows it is important to collect the sandwich structure of nanotag-NoV-LP-MNP at the center of the substrate using a magnet when dropping the sample onto the substrate.

S5 Calculation of limit of detection (LOD)

Limit of detection [4] was caculated following Eqn (2):

$$LOD = \frac{A+3.3\sigma-b}{a} \qquad (2)$$

where A, a, b, and σ denote the average and standard deviation of the control signal (blank) (n=10), average the y-intercept, and the gradient slope of the calibration line.

S6 Stability and selectivity

When a detection method is intended for practical use, high sensitivity is necessary, of course, but detection stability is becoming increasingly important. Here, three interfering solutions were prepared under the same conditions, and each solution was detected at three virus concentrations (0.1 pg, 1 pg, and 10 pg). In PBS, the CVs were 6.8%, 5.9%, and 3.6%, 5.4% on average (**Fig. S7a**). Detection in 10% and 30% human serum showed 9.3% and 6.0% on average, respectively (**Fig. S7b, c**). Pseudo-fecal samples were prepared with NoV-LP added in fecal solution (negative) and evaluated for stability. The CV values of the signals ranged from 11.2%, 9.1%, and 6.8%, 9.0% on average (**Fig. S7d**). The fact that the stability was sufficient even in the environment of fecal solution, which contains a very large number of proteins and foreign substances, suggests that this detection system has high reproducibility and stability.

To prove that the detection system is selective and can specifically detect only the target virus, the selectivity of the detection system was confirmed using various other virus samples. The NoV-LP showed significantly higher Raman scattering intensity, while other viruses showed lower values (**Fig. S7e**). This result indicates that this detection system is highly selective, using a Palmtop Raman spectrometer.

Detection sensitivity decreased by foreign impurities at all virus concentrations, and this was especially noticeable at low concentrations (**Fig. S7b–d**). Since the sandwich structure of nanotag-NoV-LP-MNP was prevented by foreign substances, the nanotag could not be separated efficiently, and the sensitivity was reduced. Comparing the sensitivity of human serum and fecal solution, the CV values of fecal solution was higher Raman intensity. There may be two possible reasons: The fecal solution contains higher than the serum solution, or, the fecal solution may contain proteolytic enzymes, which

may have degraded the NoV-LP and antibodies. The second possibility was suggested in our previous study, but the first reason is more likely because it is unclear what is contained in the fecal solution. From the above, it was found that the sensitivity of this detection system decreased at high concentrations of foreign substances. These results indicate that this detection system has relatively high sensitivity and stability not only in PBS but also in complex matrices due to the removal of nonspecific substances by magnetic separation and condensing to a single point on the substrate using a magnet.

Table S1 Specifications of Laser Raman Spectrophotometer (a) and Palmtop Raman Spectrophotometer (b)

	Laser Raman Spectrophotometer	Palmtop Raman Spectrophotometer
Laser wavelength	532, 785 nm	785 nm
Laser output	11.5 mW	5, 25, 50 mW
Objective lens magnification	×5, ×20, ×100	not installed
Wave number range	8000～50 cm^{-1}	3000～200 cm^{-1}
Spatial resolution	1 cm^{-1}/pixel	3 cm^{-1}/pixel
Main unit dimensions	880 (W) × 890 (D) × 670 (H) mm, 200 kg	85 (W) × 222 (D) ×38 (H) mm, 0.8 kg

(a)

(b)

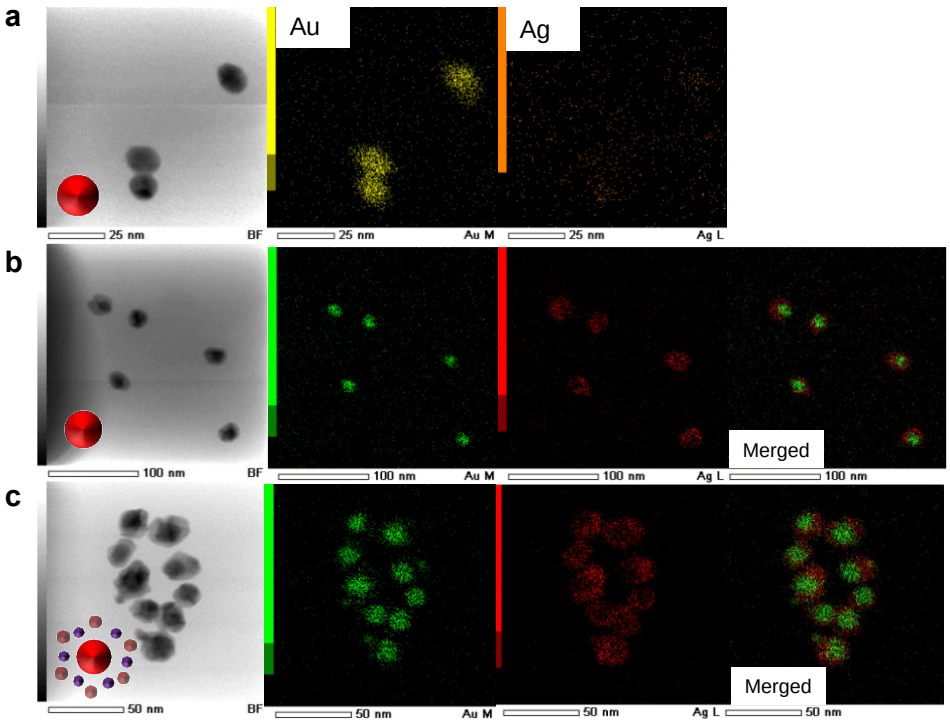

Fig. S1 Elemental analysis of AuNPs (**a**), Au@AgNPs (**b**), and Au@Ag-MBA-AuNPs (**c**)

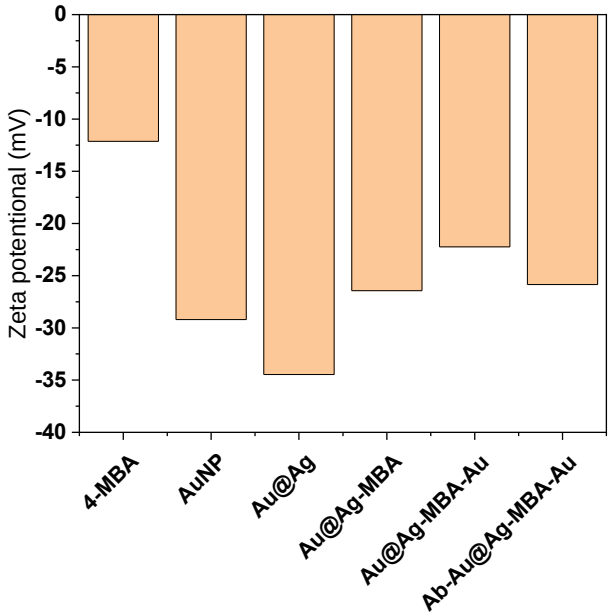

Fig. S2 Zeta potential of 4-MBA, AuNPs, Au@Ag NPs, Au@Ag-MBA NPs, Au@Ag-MBA-Au NPs, and Ab-Au@Ag-MBA-Au NPs at different synthesis steps.

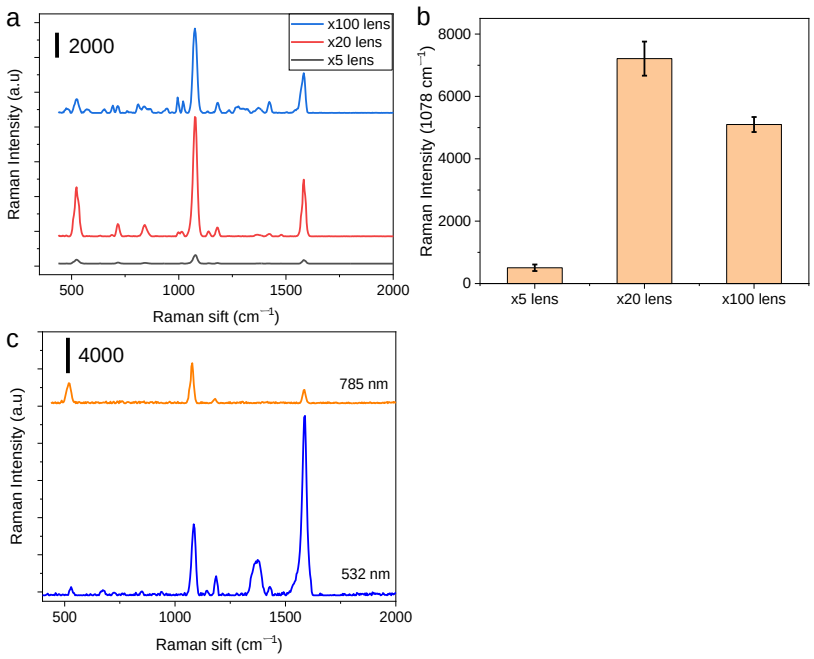

Fig. S3 Raman intensity of the laser Raman spectrophotometer. (**a**) Raman spectra by objective lens magnification (×5, ×20, and ×100), (**b**) comparison of Raman spectra at 1078 cm^{-1} by different magnification, and (**c**) comparison of Raman spectra at the objective lens magnification ×20 by different laser wavelengths.

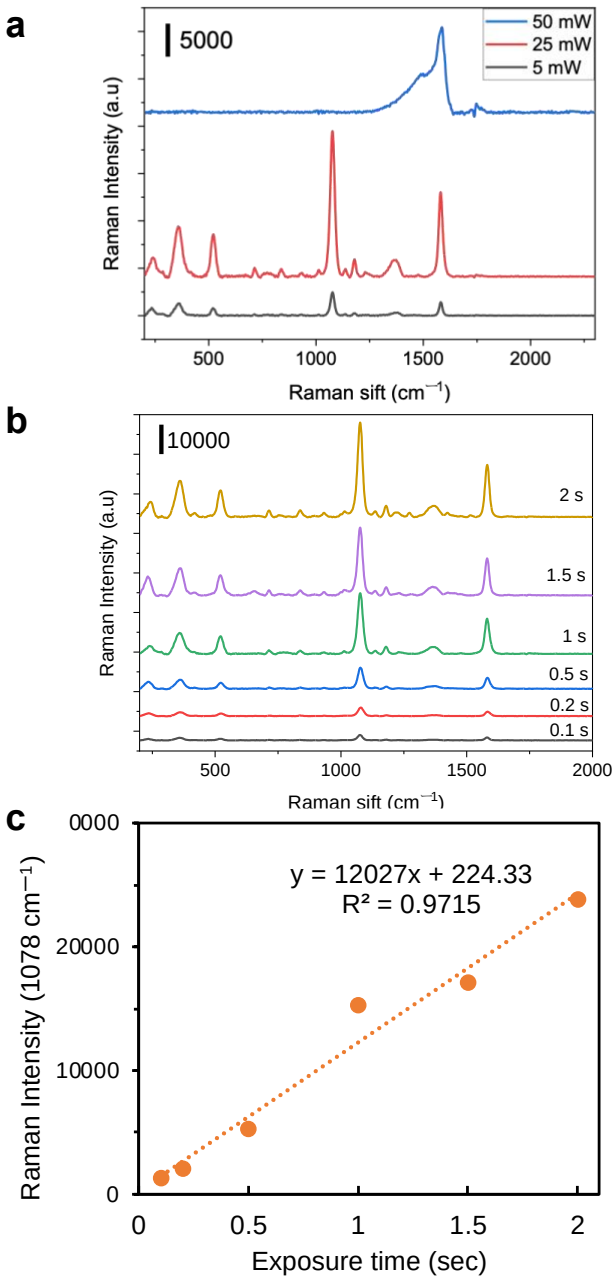

Fig. S4 Measurement conditions of Palmtop Raman spectrophotometer. (**a**) Raman intensity according to laser outputs, 5 (gray), 25 (red), and 50 (blue) mW at the laser wavelength 785 nm, (**b**) Raman intensity according to exposure time (0.1 – 2 sec) at the conditions of 785 nm of laser wavelength and 25 mW of laser output, and (**c**) exposure time-dependent Raman intensity at the conditions of wave number of 1078 cm^{-1} and laser output 25 mW.

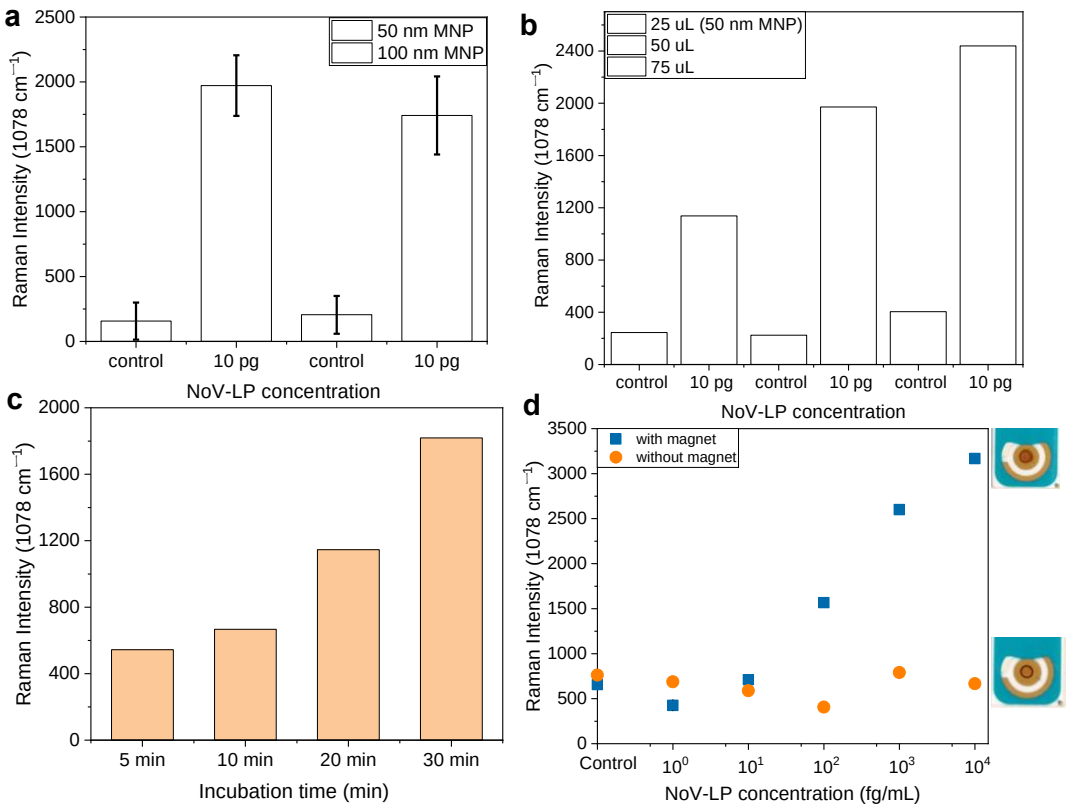

Fig. S5 Optimization of NoV-LP detection. (**a**) Effect of MNP diameter and MNP volume (**b**), and incubation time (**c**) on Raman intensity. (**d**) Raman intensity with and without a magnet when dropped on the substrate.

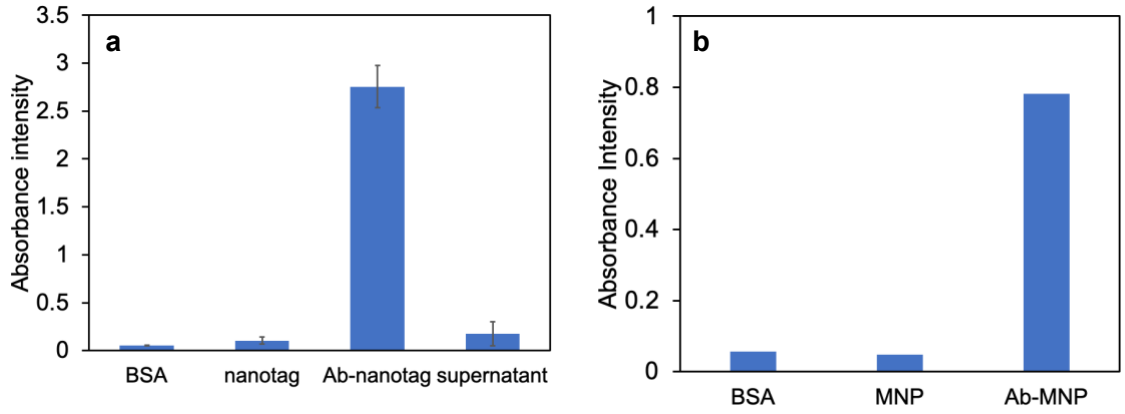

Fig. S6 Confirmation of anti-NoV antibody-conjugation on the surface of nanotag (**a**) and MNP (**b**).

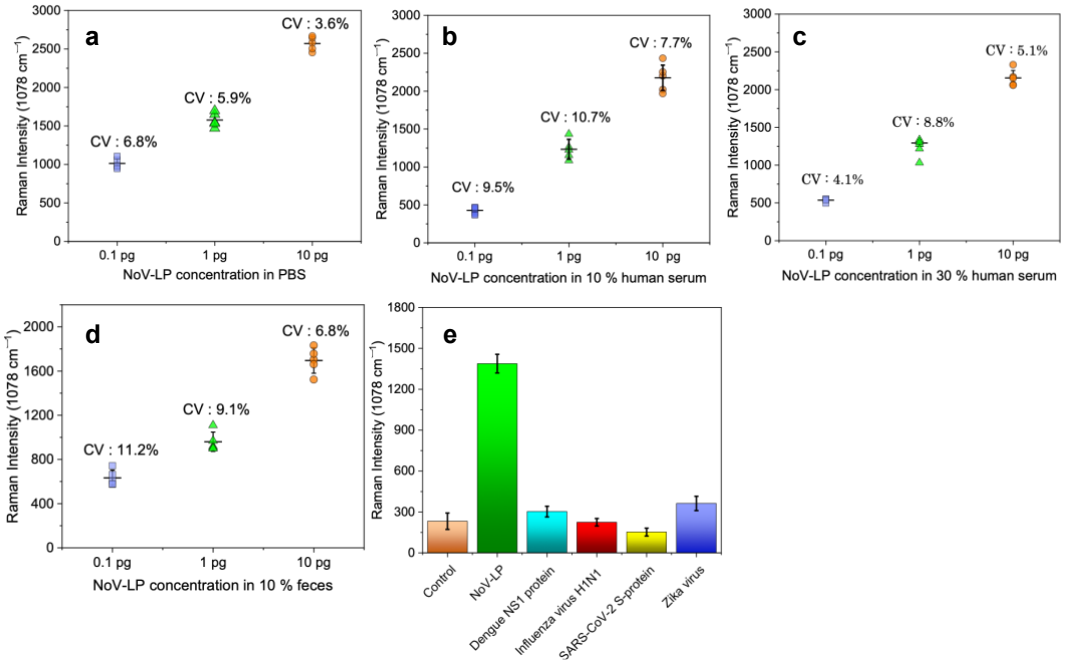

Fig. S7 Stability and selectivity test. Detection stability was examined in PBS (**a**), 10% human serum (**b**), 30% human serum (**c**), and 10% feces matrix (**d**). (**e**) One hundred pg of dengue virus NS1 protein, influenza virus H1N1, SARS CoV-2 S-protein, and zika virus, was used for selectivity test in this method. One hundred fg/mL of NoV-LP was used for positive control. Numbers in (**a–d**) denote CV values (n=5). Error bars indicate standard deviation (n=5).

References

1. Khoris IM, Takemura K, Lee J, Hara T, Abe F, Suzuki T, Park EY (2019) Enhanced colorimetric detection of norovirus using in-situ growth of Ag shell on Au NPs. Biosens Bioelectron 126:425–432. https://doi.org/10.1016/j.bios.2018.10.067
2. Luo X, Zhao X, Wallace GQ, Brunet MH, Wilkinson KJ, Wu P, Cai C, Bazuin CG, Masson JF (2021) Multiplexed SERS Detection of Microcystins with Aptamer-Driven Core-Satellite Assemblies. ACS Appl Mater Interfaces 13:6545–6556. https://doi.org/10.1021/acsami.0c21493
3. Ahmed SM, Hall AJ, Robinson AE, Verhoef L, Premkumar P, Parashar UD, Koopmans M, Lopman BA (2014) Global prevalence of norovirus in cases of gastroenteritis: a systematic

review and meta-analysis. Lancet Infect Dis 14:725–730. https://doi.org/10.1016/S1473-3099(14)70767-4

4. Khoris IM, Ganganboina AB, Suzuki T, Park EY (2021) Self-assembled chromogen-loaded polymeric cocoon for respiratory virus detection. Nanoscale 13:388-396. https://doi.org/10.1039/d0nr06893d